Experimental Proton Affinities for SiO and SiS and Their Comparison with the Proton Affinities of CO and CS Using Molecular Orbital Theory

Arnold Fox, Stanislaw Włodek, Alan C. Hopkinson, Min H. Lien, Maurice Sylvain, Christopher Rodriquez, and Diethard K. Bohme*

Department of Chemistry and Centre for Research in Experimental Space Science, York University, Downsview, Ontario, Canada M3J 1P3 *(Received: June 13, 1988)*

Gas-phase proton affinities for SiO and SiS have been determined experimentally at 295 ± 2 K by using the selected-ion flow tube (SIFT) technique with measurements of the proton-transfer kinetics for reactions of $(HOSi)^+$ and $(HSSi)^+$ with molecules having established proton affinities. The results provide proton affinities of 189.3 ± 2.6 kcal mol^{-1} for SiO and 170.3 ± 2.0 kcal mol^{-1} for SiS, enthalpies of formation at room temperature of 152.4 ± 4.6 kcal mol^{-1} for $(HOSi)^+$ and 220.8 ± 5.0 kcal mol^{-1} for $(HSSi)^+$, and bond dissociation enthalpies at room temperature of 143.4 ± 2.8 kcal mol^{-1} for $D(SiO^+-H)$ and 93.3 ± 3.0 kcal mol^{-1} for $D(SiS^+-H)$. Theory indicates that the proton affinities correspond to protonation on the heteroatom of SiO and SiS. Proton affinities for SiO and SiS have been computed at the MP4/6-31G**//6-31G** level to be 192.4 and 167.1 kcal mol^{-1} at 298 K, respectively, for protonation at the heteroatom end, and 131.8 and 154.8 kcal mol^{-1} at 298 K for protonation at the silicon atom. The bimodal proton affinities of CO, CS, SiO, and SiS are compared qualitatively by using several molecular properties computed at the 6-31G** level. Available experimental data indicate that the heteroatom-site proton affinities for organic sulfides are greater than the corresponding oxides and the theoretical oxygen and sulfur proton affinities of CO and CS concur with this general feature. Experiment and theory indicate a reversal of this trend for SiO and SiS in keeping with the more metallic property of the SiX molecules.

Introduction

The intuitive resemblance of silicon to carbon has initiated comprehensive theoretical surveys of thermochemical and structural properties of small molecules containing silicon and their carbon analogues.[1] The experimental data base for these properties is large for small molecules containing carbon but sparse for their silicon analogues. Small heteronuclear molecules containing silicon are difficult to isolate under common terrestrial conditions, especially if the silicon atom is involved in multiple bonds.[2,3]

SiO and SiS are two small molecules containing multiple bonds with silicon which are of interest in extraterrestrial environments where they have been implicated in the chemistry of dense interstellar gas clouds.[4,5] The molecules can be formed in these environments by the deprotonation of the ions $SiOH^+$ and $SiSH^+$ which are produced from the ion/molecule reactions 1 and 2.

$$Si^+ + H_2O \rightarrow SiOH^+ + H \quad (1)$$

$$Si^+ + H_2S \rightarrow SiSH^+ + H \quad (2)$$

Accurate proton affinities are required to evaluate the significance of the astrochemical deprotonation reactions for $SiXH^+$ (X = O, S) and to provide thermochemical reference data for modelling $SiXH^+/SiX$ abundance ratios in the interstellar medium.

Absolute proton affinities, while not available from experiment, have been derived theoretically for SiO and SiS for both sites of protonation,[6-9] albeit at different levels of theory and in some cases without inclusion of zero-point energies. There has not been a previous experimental study of the proton affinity of SiS. The proton affinity of SiO has been bracketed by experiment between $PA(NH_3)$ = 204.0 ± 3 kcal mol^{-1} and $PA(H_2O)$ = 166.5 ± 2 kcal mol^{-1},[1,10] but this range is too large for a meaningful comparison with the current theoretical value.

The refractory nature of SiO and SiS poses technical problems for the determination of their proton affinities by conventional equilibrium measurements. Also appearance potentials for $SiOH^+$ and $SiSH^+$ from larger, more accessible silicon containing molecules have not been reported to date.

The proton affinities of SiO and SiS have been determined experimentally in this study with the kinetic bracketing technique which relies on the observation and nonobservation of proton transfer. In principle, reaction 3 occurs spontaneously if GB(B) ≥ GB(SiX), where GB refers to gas-phase basicity. However,

$$SiXH^+ + B \rightarrow BH^+ + SiX \quad (3)$$

the sharpness of the bracketing range can be obscured by slightly endoergic proton transfer, or by kinetic factors which favour other reaction channels. For instance, a proton-transfer reaction which is endoergic by 1 kcal mol^{-1} at 295 K should attain about 9% of the collision limiting efficiency according to the empirical relationship[11]

$$k_{obsd} \simeq (0.37 \pm 0.07) k_c e^{-\Delta G^\circ/RT} \quad (4)$$

where ΔG° is the standard free energy change, k_{obsd} is the experimental reaction rate constant, and k_c is the theoretical collision rate constant. An efficiency of 100% may not be achieved until the reaction is exoergic by at least 10 kcal mol^{-1} and there is a transition region for moderately exoergic proton-transfer reactions in which the reaction efficiency is defined improperly by eq 4.[11] Also, reactions which are believed to be exoergic may not be realized unless the ergoneutral transition point has been located with sufficient certainty. The kinetic bracketing technique therefore necessitates comprehensive studies of reactions of the protonated molecule of interest with bases whose nonprotic reactions, if any, are inefficient. The absolute proton affinities of the reference bases should be well established and should lie in a bracketing range close to the proton affinity of the molecule of interest.

The experimental carbon-site proton affinities of CO and CS, the carbon analogues of SiO and SiS, are well established[11,12,19]

(1) (a) Luke, B. T.; Pople, J. A.; Krogh-Jespersen, M. B.; Apeloig, Y.; Chandrasekhar, J.; Schleyer, P. v. R. *J. Am. Chem. Soc.* **1986**, 108, 260. (b) Karni, M. *Ibid.* **1986**, *108*, 270.
(2) Raabe, G.; Michl, J. *Chem. Rev.* **1985**, *85*, 419, and references therein.
(3) Whitnall, R.; Andrews, L. *J. Am. Chem. Soc.* **1985**, *107*, 2567.
(4) Millar, T. J. *Astrophys. Space Sci., (Reidel)* **1980**, *72*, 509.
(5) Berthier, G.; Pauzat, F.; Tao, Y. Q. *Astron. Astrophys.* **1984**, *135*, L1.
(6) Tao, Y. Q.; Berthier, G.; Pauzat, F. *J. Mol. Sci. (China)* **1984**, *2*, 1.
(7) Tao, Y. Q.; Berthier, G.; Pauzat, F. *J. Mol. Sci. (China)* **1985**, *3*, 25.
(8) Berthier, G., private communication, 1987.
(9) Botschwina, P.; Rosmus, R. *J. Chem. Phys.* **1985**, *82*, 1420.
(10) Fahey, D. W.; Fehsenfeld, F. C.; Ferguson, E. E.; Viehland, L. A., *J. Chem. Phys.* **1981**, *75*, 669.
(11) Bohme, D. K.; Mackay, G. I.; Schiff, H. I. *J. Chem. Phys.* **1980**, *73*, 4976.

0022-3654/89/2093-1549$01.50/0

TABLE I: Summary of Rate Constants (10^{-9} cm^3 molecule^{-1} s^{-1}) and Product Distributions Measured for the Reactions of $SiOH^+$ at 295 ± 2 K

neutral reactant	PA[a]	products	product distribn[b]	k_{expt}[c]	k_c[d]
NH_3	204.0	$NH_4^+ + SiO$	1.0	2.5	2.2
$(CH_3)_2O$	192.1	$SiOH^+\cdot(CH_3)_2O$	0.8	0.95	1.8
		$(CH_3)_2OH^+ + SiO$	0.2		
CH_3COOH	190.2	$CH_3CO^+ + (SiO_2H_2)$	0.9	2.3	2.0
		$CH_3COOH_2^+ + SiO$	0.1		
CH_3CN	188.4	$SiOH^+\cdot CH_3CN$	0.55	0.48	4.0
		$CH_3CNH^+ + SiO$	0.45		
C_2H_5OH	188.3	$SiH_3O_2^+ + C_2H_4$	0.6	2.4	2.1
		$SiOC_2H_5^+ + H_2O$	0.3		
		$C_2H_5OH_2^+ + SiO$	0.07[e]		
		$SiH_3O^+ + C_2H_4O$	0.03[e]		
H_2CCCH_2	186.3	$SiOH^+\cdot C_3H_4$	0.8	0.031	1.2
		$C_3H_5^+ + SiO$	0.2		
CH_3OH	181.9	$SiOCH_3^+ + H_2O$	0.9	1.15	2.1
		$SiOH^+\cdot CH_3OH$	0.1		
HCOOH	178.8	$SiH_3O_2^+ + CO$	≥0.9	1.0	1.7
		$SiOH^+\cdot HCOOH$	≤0.1		
H_2S	170.2	$SiOH^+\cdot H_2S$	1.0	≤0.001	1.5

[a] The proton affinity of the neutral reactant at 298 K in kcal mol^{-1} from ref 19. Uncertainties are ±2 kcal mol^{-1} with the exception of NH_3 for which it is ±3 kcal mol^{-1}. [b] Primary product ions which contribute more than 5% (with one exception). The product distributions have been rounded off to the nearest 5% (with two exceptions) and are estimated to be accurate to ±30%. [c] The accuracy of the rate constants is estimated to be better than ±30%. The measurements were made in helium buffer gas at 0.35 Torr and 1.1×10^{16} atoms cm^{-3}. [d] The collision rate constants are derived from the combined variational transition-state theory–classical trajectory study of Su and Chesnavich (ref 18). [e] From experiments using C_2D_5OD.

and are in good agreement with values derived from theory. We explore here the extent to which theory agrees with the experimental proton affinities of SiO and SiS and the extent to which an internally consistent level of theory predicts the relative bimodal proton affinities of SiO and SiS and their carbon analogues.

Experimental Section

The measurements were performed with the selected-ion flow tube/flowing afterglow apparatus in the Ion Chemistry Laboratory of York University.[13,14] Atomic silicon precursor ions were generated by electron impact ionization of either pure $SiCl_4$ (Aldrich), SiF_4 (Matheson), or $Si(CH_3)_4$ (Stohler Isotope Chemicals), or of a 10 mol % mixture of the pure vapor in D_2 which was added to remove excited $Si(^4P)$ ions.[15] Electron energies were in the range 40–90 eV. The ions were mass selected and injected into the helium buffer gas at pressures of ca. 0.35 Torr. $SiOH^+$ and $SiSH^+$ were generated by reaction of the selected Si^+ with water vapor (ca. 2×10^{18} molecules s^{-1}) or H_2S (ca. 5×10^{17} molecules s^{-1}) introduced into the buffer gas upstream of the reaction region. In some experiments $SiOH^+$ was produced directly by electron impact ionization of $(CH_3)_3SiOH$ vapor prepared by the hydrolysis of $(CH_3)_3SiCl$ or $[(CH_3)_3Si]_2NH$.[16]

Reagent vapors were derived from HCOOH, CH_3COOH, CH_3OH (BDH Chemicals; 98, 99.7 and 99.5%, respectively), CH_3CN (MCB Chemicals, 99.6%), and C_2H_5OH (Absolute; Consolidated Alcohols). Reagent and source gases and the helium buffer gas (Matheson) were of a minimum purity of 99.5%. HCN was prepared from the reaction of NaCN with H_2SO_4.[17]

TABLE II: Summary of Rate Constants (10^{-9} cm^3 molecule^{-1} s^{-1}) and Product Distributions Measured for Reactions of $SiSH^+$ at 295 ± 2 K

neutral reactant	PA[a]	products	product distribn	k_{expt}[b]	k_c[c]
NH_3	204.0	$NH_4^+ + SiS$	1.0	0.97	2.2
HCN	171.4	$HCNH^+ + SiS$	1.0	0.61	1.6
H_2S	170.2	$H_3S^+ + SiS$	1.0	0.29	1.4
H_2O	166.5	$SiOH^+ + H_2S$	1.0	1.1	2.4
C_2H_4	162.5	$SiSH^+\cdot C_2H_4$	1.0	0.018	1.1

[a] The proton affinity of the neutral reactant at 298 K in kcal mol^{-1} from ref 19. Uncertainties are ±2 kcal mol^{-1} with the exception of NH_3 for which it is ±3 kcal mol^{-1}. [b] The accuracy of the rate constants is estimated to be ±30%. The measurements were made in helium buffer gas at 0.35 Torr and 1.1×10^{16} atoms cm^{-3}. [c] Collision rate constants are derived from the combined variational transition-state theory–classical trajectory study of Su and Chesnavich (ref 18).

Results

Experimental Proton Affinities. Tables I and II summarize the measured rate coefficients, calculated collision rate coefficients[18] and product distributions obtained in this study. Each summary lists all of the primary product ions that were observed to contribute more than 5% to the total product spectrum with one exception. The reactions are listed in order of decreasing proton affinity of the neutral substrate.[19] Rate coefficients were derived in the usual manner[13] and product distributions were derived by the method of Adams and Smith.[20] Rate coefficients for important secondary reactions were obtained by fitting the integrated rate expressions to the product ion profiles. The reacting isomers of $SiOH^+$ and $SiSH^+$ were found to be those with protonation on O and S, respectively.

Reactions of $SiOH^+$. The results obtained for reactions of $SiOH^+$ are summarized in Table I. Results for reactions with CH_3COOH, C_2H_5OH, CH_3OH, and HCOOH have been discussed elsewhere.[15]

NH_3. Ammonia was observed to react efficiently by proton transfer and NH_4^+ was the only primary product ion observed. The rate constant for proton transfer, 2.5×10^{-9} cm^3 molecule^{-1} s^{-1}, is in good agreement with the value of 2.0×10^{-9} cm^3 molecule^{-1} s^{-1} obtained by Fahey et al. under similar experimental conditions.[10]

$(CH_3)_2O$. The $SiOH^+$ reacted with dimethyl ether to generate the adduct ion $SiOH^+\cdot(CH_3)_2O$ and protonated dimethyl ether in a ratio of 4 to 1, respectively. Account was taken of the small contribution (<8%) to the formation of protonated dimethyl ether from impurity H_3O^+ ions. The adduct ion appeared primarily as the hydrate $SiOH^+\cdot(CH_3)_2O\cdot H_2O$ because of the presence in the reaction region of the water vapor injected upstream to form $SiOH^+$. The rate constant for the depletion of $SiOH^+$ was determined to be 9.5×10^{-10} cm^3 molecule^{-1} s^{-1} at a total pressure of 0.35 Torr and helium density of 1.1×10^{16} atoms cm^{-3}. The adduct ion did not appear to react further with dimethyl ether but its hydrate underwent a slow switching reaction to generate the bis adduct ion, $SiOH^+\cdot((CH_3)_2O)_2$. The bimolecular rate constant for the latter was found to be 6.4×10^{-11} cm^3 molecule^{-1} s^{-1} by fitting the observed growth and decay of the mono adduct hydrate ion with an integrated rate expression.

$H_3SiO_2^+$ and $H_5SiO_3^+$ were present initially as impurity ions at levels less than 10% of the $SiOH^+$ signal and were observed to decay with the addition of dimethyl ether. Both of these ions could contribute to the formation of $SiOH^+\cdot(CH_3)_2O\cdot H_2O$ (by association and switching, respectively), but the majority of the

(12) Smith, D.; Adams, N. G. *J. Phys. Chem.* **1985**, 89, 3964.
(13) Mackay, G. I.; Vlachos, G. D.; Bohme, D. K.; Schiff, H. I. *Int. J. Mass Spectrom. Ion Phys.* **1980**, 36, 259. Details of the calculation of bimolecular rate constants from our experimental data are given by: Bohme, D. K.; Hemsworth, R. S.: Rundle, H. W.; Schiff, H. I. *J. Chem. Phys.* **1973**, *58*, 3504.
(14) Raksit, A. B.; Bohme, D. K. *Int. J. Mass Spectrom. Ion Phys.* **1983**, *55*, 69.
(15) Włodek, S.; Fox, A.; Bohme, D. K. *J. Am. Chem. Soc.* **1987**, *109*, 6663.
(16) (a) Sommer, L. H. *Stereochemistry, Mechanism and Silicon*; McGraw-Hill: New York, 1965; p 78. (b) Sauer, R. O. *J. Am. Chem. Soc.* **1944**, *66*, 1707.
(17) Glemser, O. In *The handbook of preparative inorganic chemistry*; Brauer, G., Ed.; Academic Press: New York, 1963; p 658.
(18) Combined variational transition state theory-classical trajectory study of: Su, T.; Chesnavich, W. J. *J. Chem. Phys.* **1982**, *76*, 5183.
(19) (a) Lias, S. G.; Liebman, J. F.; Levin, R. D. *J. Phys. Chem. Ref. Data* **1984**, *13*, 695. (b) Lias, S. G., private communication, 1987.
(20) Adams, N. G.; Smith, D. *J. Phys. B* **1976**, *9*, 1439.

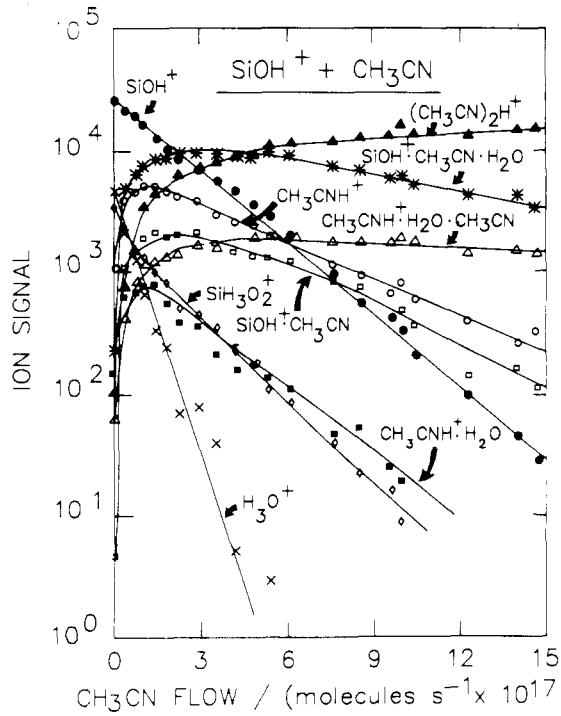

Figure 1. The observed variation of ion signals recorded for the addition of methyl cyanide vapor into the reaction region of the SIFT apparatus in which $SiOH^+$ is initially established as the dominant ion in helium buffer gas. $P = 0.33$ Torr, [He] = 1.07×10^{16} atoms cm^{-3}, $\bar{v} = 6.85 \times 10^3$ cm s^{-1}, and $T = 297$ K. $SiOH^+$ was derived from the reaction of $Si^+(^2P)$ with water vapor.

observed decays of their ion signals could be attributed to the depletion of their precursor ion $SiOH^+$ in the reaction region.

The apparent reactivity of a majority of the adduct ions $SiOH^+ \cdot (CH_3)_2O$ toward H_2O and the nonreactivity of a minority of the adduct ions toward $(CH_3)_2O$ is curious. One possible explanation involves the formation of two isomeric forms of the adduct ion. One adduct could involve strong hydrogen bonding in the configuration $[SiO \cdot H \cdot O(CH_3)_2]^+$ for which additional attachment to water or (through switching) to dimethyl ether would need to occur at the silicon. A different adduct could be formed by insertion of the silicon end of $SiOH^+$ into the C–O bond of dimethyl ether to form the cation $[CH_3 \cdot SiOH \cdot OCH_3]^+$ in a manner encountered previously for reactions of Si^+ with alcohols and acids.[15] The affinity of this trivalent siliconium adduct ion to further complexation with water or dimethyl ether probably would involve hydrogen bonding through the OH substituent on silicon.

CH_3CN. The $SiOH^+$ reacted with CH_3CN to generate protonated methyl cyanide and the adduct ion $SiOH^+ \cdot CH_3CN$ in about equal amounts at 0.33 Torr and 1.1×10^{16} helium atoms cm^{-3}. The observations made in one experiment are shown in Figure 1. The adduct ion $SiOH^+ \cdot CH_3CN$ appeared mainly as the adduct $SiOH^+ \cdot CH_3CN \cdot H_2O$ because of its association reaction with the water vapor introduced upstream to generate $SiOH^+$. The product distribution was corrected for the contribution to CH_3CNH^+ due to the proton-transfer reaction with the H_3O^+ initially present as an impurity ion. $SiH_3O_2^+$ was also present initially as an impurity ion due to the association reaction of $SiOH^+$ with water vapor. The decay of this ion seen in Figure 1 can be attributed primarily to the depletion of the $SiOH^+$ precursor in the reaction region. Also it appears that the $SiH_3O_2^+$ entering the reaction region associates with CH_3CN and so contributes to the ion signal due to $SiOH^+ \cdot CH_3CN \cdot H_2O$ formed from $SiOH^+ \cdot CH_3CN$.

H_2CCCH_2. The $SiOH^+$ was generated by direct electron impact ionization of trimethylsilanol and was observed to react slowly with allene, $k = 3.1 \times 10^{-11}$ cm^3 $molecule^{-1}$ s^{-1}, to form the adduct ion $SiOH^+$-allene, and protonated allene in a 4:1 ratio, respectively, at 0.33 Torr and 1.1×10^{16} He atoms cm^{-3}. A trace amount, ≤3%, of a primary product ion was observed at m/z 59 which may be $SiOCH_3^+$. Two molecules of allene were observed to add to the primary product ions $C_3H_5^+$ and $SiOH^+ \cdot C_3H_4$ to form $C_3H_5^+ \cdot (C_3H_4)_{1,2}$ and $SiOH^+ \cdot (C_3H_4)_{2,3}$ by sequential, presumably termolecular, association reactions.

H_2S. There was no measurable reaction between $SiOH^+$ and H_2S, $k \leq 1 \times 10^{-12}$ cm^3 $molecule^{-1}$ s^{-1}, although traces of the adduct $SiOH^+ \cdot H_2S$ were observed. Some H_3S^+ was seen to be produced but it was ascribed entirely to the impurity H_3O^+ ions.

Reactions of $SiSH^+$. Results obtained for the reactions of $SiSH^+$ are summarized in Table II.

NH_3, HCN, and H_2S. The only channel observed for the reactions of $SiSH^+$ with these molecules was proton transfer. The secondary reactions initiated by the protonated molecules are well established.

H_2O. Proton transfer was not observed in the reaction of $SiSH^+$ with water vapor. $SiOH^+$ was generated instead. The reaction is likely to proceed by insertion of the silicon end of ^+SiSH into O–H with loss of H_2S, or by parallel alignment of ^+SiSH with H_2O as depicted in I.

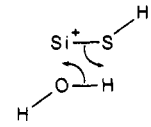

I

C_2H_4. Association to form the adduct ion $SiSH^+ \cdot C_2H_4$ was the only channel observed in the reaction of $SiSH^+$ with ethylene. The effective bimolecular rate constant was found to be 1.77×10^{-11} cm^3 $molecule^{-1}$ s^{-1} at a helium buffer concentration of 1.14×10^{16} atoms cm^{-3}.

Proton Affinities. Insignificant proton transfer was observed for the reactions of $SiOH^+$ with the selected molecules having proton affinities equal to or less than the proton affinity of methanol. This result suggests that PA(SiO) > PA(CH_3OH). Some proton transfer was observed in the reaction with allene which might imply that PA(SiO) < PA(allene). However, the overall efficiency of the reaction is only 0.026 and proton transfer competes with adduct formation. Proton transfer and adduct formation also compete in the reaction of $SiOH^+$ with CH_3CN. The overall efficiency for this latter reaction, 0.12, is less then the threshold efficiency. 0.37 ± 0.07, expected from eq 4 for ergoneutral reactions. The proton-transfer reactions of $SiOH^+$ with allene and CH_3CN are therefore both endoergic. We estimate the efficiency for proton transfer with CH_3CN to lie between 0.12 and 0.06 depending on whether or not the competing channel leading to adduct formation converts to proton transfer in the absence of collisional stabilization. For example, axial addition of the bipolar O-protonated silicon oxide to the N atom of CH_3CN could form the association complex $[HOSi \cdot NCCH_3]^+$ or $[SiOH \cdot NCCH_3]^+$ which, in the absence of interconversion, may lead independently to a collisionally stabilized adduct ion and protonated acetonitrile, respectively. With an efficiency between 0.06 and 0.12, the empirical eq 4 leads to a slight endoergicity for the proton-transfer reaction of $SiOH^+$ with CH_3CN with a value between 0.54 and 1.24 kcal mol^{-1} at 298 K. The efficiency for proton transfer with allene lies between 0.026 and 0.005 and the application of eq 4 leads to an endoergicity for proton transfer between 1.45 and 2.63 kcal mol^{-1} at 298 K. We can use these ranges in endoergicity to estimate a range in the proton affinity difference between SiO and these two references bases, viz., allene and CH_3CN, and therefore an absolute proton affinity for SiO.

No complications due to a competing channel exist in the case of the proton-transfer reactions of $SiSH^+$. For the reactions of $SiSH^+$ the results in Table II show a clear trend of decreasing efficiency for proton transfer with decreasing proton affinity. No proton transfer was observed with molecules having proton affinities below that of H_2S so that the efficiency of the proton-transfer reaction with H_2S was chosen in the determination the proton affinity of SiS. In this case the efficiency is 0.21 and there are no competing channels. Equation 4 provides a standard free energy change at 298 K between 0.22 and 0.45 kcal mol^{-1}.

TABLE III: Molecular Properties for the Singlet Ground States of CO, CS, SiO, and SiS Computed at the 6-31G Level of Optimized Geometry**

molecule (site of protonatn)	α^a	$\Delta q_T{}^b$ (Δq_s)^f	$\mu_D{}^c$	$E_{1s}{}^d$	$E_\sigma{}^e$	$E_\pi{}^e$
CO (C)	1.778 (∥)	0.55 (0.19)	0.264	−11.355	−0.5459	−0.63925
CO (O)	1.778 (∥)	0.45 (0.42)	0.264	−20.675	−0.5459	−0.63925
CS (C)	4.776 (∥)	0.65 (0.60)	−1.34	−11.351	−0.4673	−0.46338
CS (S)	2.018 (⊥)	0.79 (0.33)	−1.34	−91.986	−0.4673	−0.46338
SiO (Si)	3.751 (∥)	0.88 (0.23)	3.25	−68.804	−0.4321	−0.4748
SiO (O)	3.751 (∥)	0.59 (0.54)	3.25	−20.539	−0.4321	−0.4748
SiS (Si)	8.845 (∥)	0.97 (0.47)	2.44	−68.828	−0.3919	−0.3913
SiS (S)	3.915 (⊥)	0.84 (0.53)	2.44	−91.929	−0.3919	−0.3913

[a] Molecular static electric dipole polarizabilities of the neutral bases in Å^3 calculated from the second derivative of energy with respect to an applied uniform electric field parallel or perpendicular to the molecular axis depending upon the geometry of the protonated molecule (M. Sylvain, University of Toronto). [b] Amount of electron density transferred from the base to the proton using the Mulliken charge distribution of the protonated species given in Figure 2. [c] Calculated permanent dipole moment in debye. [d] Computed core 1s orbital binding energy (in hartrees) of the protonated atom in the neutral. [e] Energies (in hartrees) of the highest occupied molecular orbital of σ symmetry (σ-HOMO) and of π symmetry (π-HOMO). [f] Negative charge transferred from the substituted atom of the base subsequent to protonation of the alternate site.

To convert changes in standard free energy to changes in standard enthalpy the standard entropy changes for the proton-transfer reactions are assumed to be determined approximately by the changes in the rotational symmetry numbers of the reactants and products according to eq 5 which applies to reaction 3:

$$\Delta S^\circ = R \ln [\sigma(\mathrm{SiXH^+})\sigma(\mathrm{B})/\sigma(\mathrm{SiX})\sigma(\mathrm{BH^+})] \qquad (5)$$

For the proton-transfer reactions of $SiOH^+$ with CH_3CN and allene and of $SiSH^+$ with H_2S, eq 5 predicts standard entropy changes of 0, 1.38,[21] and −0.81 cal mol^{-1} deg^{-1}, respectively. The corresponding changes in standard enthalpy (and differences in proton affinity) become equal to a value between 0.54 and 1.24 kcal mol^{-1} with respect to PA(CH_3CN), a value between 1.86 and 3.04 kcal mol^{-1} with respect to PA(allene), and a value between −0.02 and +0.21 kcal mol^{-1} with respect to PA(H_2S), respectively.

The proton affinities of CH_3CN, allene, and H_2S at 298 K are 188.4 ± 2, 186.3 ± 2, and 170.2 ± 1.7 kcal mol^{-1}, respectively.[19,22] With the differences in proton affinity indicated above, these lead to a proton affinity for SiO in the range from 186.9 to 191.6 kcal mol^{-1} with respect to PA(CH_3CN) and in the range from 186.1 to 191.3 with respect to PA(allene). The slightly smaller range in proton affinity associated with proton transfer to CH_3CN favours acetonitrile as the anchor of choice and leads to a final experimental proton affinity for SiO of 189.3 ± 2.6 kcal mol^{-1} when account is also taken of the uncertainty of 0.4 kcal mol^{-1} associated with the determination of the rate constant and product branching. The final experimental proton affinity similarly arrived at for SiS is 170.3 ± 2.0 kcal mol^{-1}.

The experimentally derived standard enthalpies of formation for SiO and SiS,[23,24] together with the standard enthalpy of formation of the proton[19] lead to standard enthalpies of formation for $SiOH^+$ and $SiSH^+$ of 152.4 ± 4.6 and 220.8 ± 5.0 kcal mol^{-1}, respectively, at 298 K.

Theoretical Molecular Properties and Proton Affinities. The GAUSSIAN 82 software[25] was used to compute the closed-shell

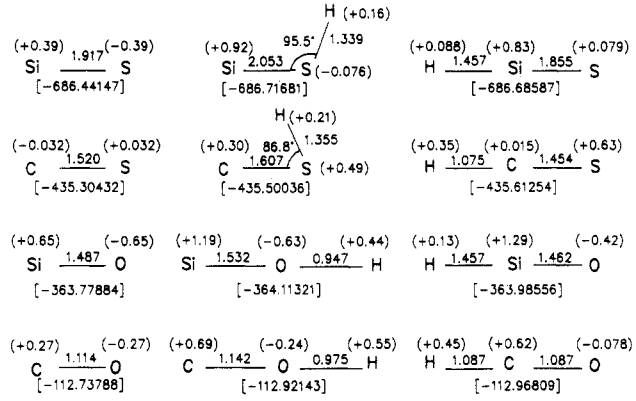

Figure 2. Optimized geometries of bases and their protonated molecular ions at the SCF level using 6-31G** basis sets. Parentheses contain net Mulliken charges condensed to atoms. Bond lengths are given in angstroms. The effective electronic energy (in hartrees) is given in square brackets.

TABLE IV: Closed-Shell MP4/6-31G//6-31G** Effective Electronic Energies (E_{el}), Vibrational Energies at 298 K, and Computed Proton Affinities for SiO and SiS at 298 K**

molecule	E_{el}/hartrees	$E^{298}{}_v{}^a$	PA^{298}
SiO	−364.064 49	2.016	
$SiOH^+$	−364.378 95	8.436	192.4
$HSiO^+$	−364.280 29	7.358	131.6
SiS	−686.666 93	1.212	
$SiSH^+$	−686.938 88	5.951	167.1
$HSiS^+$	−686.919 71	6.474	154.8

[a] Vibrational energy at room temperature in kcal mol^{-1} based on frequencies obtained at the SCF level.

electronic energies (E_{el}) of the molecules CO, $(HCO)^+$, $(COH)^+$, CS, (HCS^+), $(CHS)^+$, SiO, $(HSiO)^+$, $(SiOH)^+$, SiS, $(HSiS)^+$, and $(SiSH)^+$. The geometry of each molecule was optimized by using the 6-31G** basis set. The results are summarized in Figure 2 along with the net Mulliken charges condensed to atoms and the effective electronic energy of each configuration. Protonation at the sulfur and oxygen site of each neutral base leads to a bent and linear structure, respectively. Protonation at the carbon and silicon sites incur shorter CX and SiX bonds, while the converse is true for protonation at X. The latter result is consistent with

(21) The ground state of protonated allene belongs to the C_{2v} point group. Raghavachari, K.; Whiteside, R. A.; Pople, J. A.; Schleyer, P.v.R, *J. Am. Chem. Soc.* **1981**, *103*, 5649. Allene belongs to the D_{2d} point group. Hopkinson, A. C.; Lien, M. H. *J. Chem. Phys.* **1977**, *67*, 517.

(22) Tanaka, K.; Mackay, G. I.; Bohme, D. K. *Can. J. Chem.* **1978**, *56*, 193.

(23) Rosenstock, H. M.; Draxl, K.; Steiner, B. W.; Herron, J. T. *J. Phys. Chem. Ref. Data* **1977**, *6*, Suppl. 1.

(24) Chase Jr., M. W.; Davies, C. A.; Downey Jr., J. R.; Frurip, D. J.; McDonald, R. A.; Syverud, A. N. *J. Phys. Chem. Ref. Data* **1985**, 14, Suppl. 1.

(25) Binkley, J. S.; Frisch, M. J.; Raghavachari, K.; DeFrees, D. J.; Schlegel, H. B.; Whiteside, R.; Fluder, E.; Seeger, R.; Pople, J. A. GAUSSIAN 82, Release A, Carnegie-Mellon University, Pittsburgh, PA.

the qualitative notion of a shift of non-bonding electron density from O and S into the CX and SiX bonds for proton attachment at C and Si, or away from these bonds upon protonation at X. Table III presents additional molecular information on polarizabilities, charge transfer to the proton, dipole moments, core 1s orbital binding energies, and energies for the highest occupied orbitals of σ and π symmetry of the neutral molecules.

Electron correlation energies for the most stable SCF configurations of the silicon species were calculated at the MP4 level in order to derive proton affinities. The results are summarized in Table IV. The proton affinities were computed according to eq 6

$$PA(SiX) = -\Delta E^0_{el} - \Delta E^0_v - \Delta(\Delta E^{298}_v) - \Delta E^{298}_r + (5/2)RT \quad (6)$$

where ΔE^0_{el} is the effective electronic energy change for the process

$$SiX + H^+ \rightarrow (SiX)H^+ \quad (X = O, S) \quad (7)$$

ΔE^0_v and $\Delta(\Delta E^{298}_v)$ are the zero-point vibrational and room temperature vibrational energy differences, respectively, and ΔE^{298}_r is the rotational energy difference at 298 K. $(5/2)RT$ corresponds to the sum of the $\Delta(PV)$ work term and the translational energy of the proton.

Discussion

Experimental Proton Affinities. Our determination of the proton affinity for SiO by kinetic bracketing, 189.3 ± 2.6 kcal mol^{-1} at 295 ± 2 K, has greatly reduced the previous uncertainty of 42.5 kcal mol^{-1} in the experimental proton affinity for this species.[10] Our kinetically bracketed proton affinity for SiS, 170.3 ± 2.0 kcal mol^{-1} at 295 ± 2 K, is the first experimentally measured proton affinity for this molecule to be reported. Experimental thermochemical properties for the higher energy isomers $HSiO^+$ and $HSiS^+$ have not yet appeared in the literature, to the best of our knowledge.

The experimental carbon-site proton affinities of the carbon analogues, CO and CS, are also well established. The former has been established from equilibrium constant and appearance potential measurements to be 141.9 kcal mol^{-1},[19] while that for CS, 188.2 ± 1 kcal mol^{-1} at 300 K, has been measured recently by using the kinetic bracketing technique.[12] Thus the experimental proton affinity for CO lies 47.4 ± 2.6 kcal mol^{-1} below the oxygen-site proton affinity for SiO while that for CS lies 17.9 ± 3.0 kcal mol^{-1} above the sulfur-site proton affinity for the silicon analogue SiS. The oxygen-site proton affinity for CO has recently been reported to be 102 ± 2 kcal mol^{-1} at 303 K which lies 87.3 ± 4.6 kcal mol^{-1} below that for SiO.[26] A reliable experimental enthalpy for deprotonation of the higher energy isomer CSH^+ is not yet available.

Experimental Reactivities. $SiOH^+$ and HCO^+. Proton transfer is observed for reactions of $SiOH^+$ with bases having proton affinities ≥186.3 kcal mol^{-1} at 296 ± 2 K. With few exceptions, other bimolecular channels among reactions studied with bases having proton affinities in this range and for which established thermochemical data are available can be shown to be endothermic. An upper limit of 162.2 kcal mol^{-1} is obtained for the enthalpy of formation of $SiOCH_3^+$ formed in the reaction of $SiOH^+$ with methanol. It conforms with a semiempirical enthalpy of formation for this ion of 149 ± 3 kcal mol^{-1}.[27a,b] The latter value suggests that the generation of $SiOCH_3^+$ from dimethyl ether may be exothermic by as much as 7 kcal mol^{-1} so that its non-appearance may owe to unfavorable kinetic factors. Similarly, a possible minor generation of $SiOCH_3^+$ from allene may be thermoneutral if the vinylidene by-product isomerizes to acetylene with negligible activation energy.[27c] The observed generation of $SiH_3O_2^+$ from the dehydration of ethanol and formic acid implies an enthalpy of formation for this ion ≤83.7 kcal mol^{-1} which makes its production from dimethyl ether also exothermic by at least 12 kcal mol^{-1}. This channel is expected to be kinetically unfavorable owing to the requirement of considerable skeletal rearrangement.

When proton transfer is moderately endothermic or kinetically disfavored, bimolecular insertion pathways which implicate the silene character of this ion are observed for the reactions of $SiOH^+$ with CH_3COOH, C_2H_5OH, CH_3OH, and HCOOH.[15] These same molecules, as well as all the others listed in Table I, react with the configurationally dissimilar HCO^+ ion usually by proton transfer and, occasionally, by dissociative proton transfer.[28] Since the proton affinity of the carbon site of CO lies 47 kcal mol^{-1} below that of SiO, these observations are not entirely unexpected. The failure to observe CH_3OC^+ or CH_3CO^+ from the reaction of HCO^+ with CH_3OH (ΔH^0_{rxn} = −4 and −56 kcal mol^{-1}, respectively)[24,29] by analogy with the observed generation of $SiOCH_3^+$ from the reaction of $SiOH^+$ with CH_3OH can be attributed to a combination of the noninsertive character of HCO^+ and competitive energetics for proton transfer. Adduct formation involving HCO^+ and base molecules has not been observed and would not be anticipated since carbon is not an effective partner for hydrogen bonding.

$SiSH^+$ and HCS^+. Proton transfer is the only reaction channel observed for the reactions of $SiSH^+$ with molecules whose proton affinities exceed 170.2 kcal mol^{-1} (see Table II). The silene character of this ion is evident in the bimolecular reaction of $SiSH^+$ with water vapor (exothermic by 14 kcal mol^{-1} at room temperature). On the other hand, generation of $SiNH_2^+$ from the insertion of $SiSH^+$ into NH_3 is thermoneutral given a heat of formation at 298 K of 214.2 kcal mol^{-1} [30] and was not observed. The failure to observe this channel must therefore be attributed to a kinetic barrier. In contrast to the reactions of $SiOH^+$, the reactions of $SiSH^+$ did not exhibit adduct formation except for the slow appearance of $SiSH^+ \cdot C_2H_4$ which was observed as the only product in the reaction of $SiSH^+$ with C_2H_4. Adduct formation is probably unfavorable in general because of the inability of sulfur to sustain strong hydrogen bonds. Sulfur has a smaller nominal electronegativity than oxygen or nitrogen and the ion $H_5S_2^+$ did not appear in any of these experiments in spite of the common presence of H_3S^+ and H_2S vapor injected upstream of the reaction region of the flow tube. Moreover, the bent geometry of $SiSH^+$ (Figure 2) may render proton transfer sterically more facile for initial alignments which favor silicon-end attachment.

HCS^+ is isostructural with HCO^+ and its reactivity with a series of molecules ranging in basicity from CO to NH_3 has been investigated by Smith and Adams.[12] Proton transfer was observed to be ubiquitous for the reactions of this ion with bases whose proton affinities exceed 187.4 kcal mol^{-1}, while less basic molecules did not appear to react at all with HCS^+. The proton affinity of the carbon site of CS is 46 kcal mol^{-1} greater than that of CO and much less excess energy is available for dissociative proton transfer. As with HCO^+, adduct formation was not observed with HCS^+.[12]

A direct comparison of the reactions of $SiSH^+$ and HCS^+ with water cannot be made since the generation of HCO^+ from HCS^+ and water analogous to the generation of $SiOH^+$ from $SiSH^+$ and water is endothermic by 8.2 kcal mol^{-1}. However, the reaction of HCS^+ with CH_3SH, the analogue of the reaction of $SiOH^+$ with CH_3OH, only generated the protonated base.[12] The proton transfer is endothermic by 0.8 kcal mol^{-1} while the unobserved

(26) Freeman, C. G.; Knight, J. S.; Love, J. G.; McEwan, M. J. *Int. J. Mass Spectrom. Ion Processes* **1987**, *80*, 255.

(27) (a) Singlet ground-state optimized geometries and room temperature vibrational energies for the linear ions $SiOCH_3^+$ and CH_3SiO^+, and the fragments SiO and CH_3^+ were computed using the 6-31G* basis set. Effective electronic energies derived for these species at the MP2/6-31G**//6-31G* level with the experimental heats of formation of CH_3^+ and SiO at 298 K (ref 24 and 27b) and usual thermodynamic corrections lead to $\Delta H_f°_{298}(SiOCH_3^+)$ = 149 ± 3 kcal mol^{-1} and $\Delta H_f°_{298}(CH_3SiO^+)$ = 178 ± 3 kcal mol^{-1}. (b) Traeger, J. C.; McLoughlin, R. G. *J. Am. Chem. Soc.* **1981**, *103*, 3647. (c) Krishnan, R.; Frisch, M. J.; Pople, J. A.; Schleyer, P. v. R. *Chem. Phys. Lett.* **1981**, *79*, 408.

(28) Tanner, S. D.; Mackay, G. I.; Hopkinson, A. C.; Bohme, D. K. *Int. J. Mass Spectrom. Ion Phys.* **1979**, *29*, 153.

(29) Nobes, R. H.; Bouma, W. J.; Radom, L. *J. Am. Chem. Soc.* **1983**, *105*, 309.

(30) Wlodek, S.; Rodriquez, C. F.; Lien, M. H.; Hopkinson, A. C.; Bohme, D. K. *Chem. Phys. Lett.* **1988**, *143*, 385.

generation of CH_3CS^+, the analogue of $SiOCH_3^+$, should be exothermic by at least 13.5 kcal mol^{-1}.[31] The failure to observe CH_3CS^+ or any of its isomers is consistent with the noninsertive carbonium ion character of HCS^+. Generation of HCO^+, H_2CS^+, S_2^+, and HS^+ from bimolecular reactions of HCS^+ with H_2CO and H_2S both of which have proton affinities which underlie 188.2 kcal mol^{-1}, can be shown to be endothermic. HCS^+ has been shown to be unreactive toward H_2CO.[12]

Theoretical Proton Affinities. SiO and SiS. Our computed heteroatom proton affinities for SiO and SiS given in Table IV lie within +3.1 and −3.2 kcal mol^{-1}, respectively, of the average experimental values determined in this study. The theoretically derived proton affinities of these molecules for proton attachment to silicon, 131.6 and 154.8 kcal mol^{-1}, respectively, suggest that proton transfer should be exothermic for the reactions of $HSiO^+$ and $HSiS^+$ with molecules within the basicity ranges from H_2O to CH_3OH and from C_2H_4 to H_2O, respectively. Our failure to observe these proton-transfer reactions implies that the ions under study were $SiOH^+$ and $SiSH^+$ and not $HSiO^+$ and $HSiS^+$. This is not surprising since formation of $HSiO^+$ from the reaction of $Si^+(^2P)$ with water is endothermic by 26 kcal mol^{-1} while the formation of $HSiS^+$ from the reaction of $Si^+(^2P)$ with H_2S is exothermic by only 7 kcal mol^{-1} compared to an exothermicity of 19 kcal mol^{-1} for the formation of $SiSH^+$.

CEPA-1 calculations of Botschwina and Rosmus have shown the O-end proton affinity of SiO to be 194.6 kcal mol^{-1} at 0 K.[9] This value can be adjusted to 195.8 kcal mol^{-1} at 298 K by using their normal anharmonically corrected vibrational frequencies for SiO and $SiOH^+$ provided at the same level and the usual thermodynamic corrections. Surprisingly, this value is slightly less accurate than our room temperature proton affinity for this molecule computed at the MP4 correlation level and incorporating SCF harmonic vibrational frequencies. On the other hand, the S-atom proton affinity of SiS computed from DZDP basis sets and limited configuration interaction is coincident, perhaps fortuitously, with our experimental value when SCF zero-point vibrational energies and the usual thermal corrections to 298 K are applied.[7,8]

CO and CS. The computed proton affinities of carbon monoxide are 143.2 and 102.8 kcal mol^{-1} for carbon and oxygen protonation, respectively, at 298 K, using 6-311/G** (2df,2pd) wave functions correlated at the MP4 level.[32] The latter value is consistent with the observation of inefficient proton transfer from COH^+ to H_2.[26]

The CEPA-1 computed carbon-end proton affinity of CS at 0 K, 189.5 ± 1.2 kcal mol^{-1} is in good agreement with experiment and a value of approximately 115.4 ± 1 kcal mol^{-1} at 298 K can be derived for CS protonated on sulfur by using the MRD CI calculations of Pope et al.[12,33]

Qualitative Comparisons of Proton Affinities. There is good to excellent agreement between the results of high-level ab initio molecular orbital calculations and the experimental determinations of the normal proton affinities of SiO, SiS, CO, and CS. However, a qualitative treatment of physical causes underlying the relationships of all of these proton affinities remains to be addressed.

A semiquantitative treatment of the relative proton affinities of SiO, SiS, CO, and CS which invokes the calculated electrostatic potential, $V(r)$, in the space surrounding these molecules recently has been proposed by Pauzat et al.[34] The magnitudes and positions of the electrostatic potential minima successfully reflect the preferred site of proton attachment for each base and the approximate geometry of each protonated molecule. Also, a direct comparison of the depths of the electrostatic potential minima of several pairs of bases predicts the correct ordering of their proton affinities, viz. SiO(O) > SiS(S), SiO(O) > CO(O), CS(C) > CO(C), and CS(C) > SiS(S), where proton attachment occurs at the atom in parentheses. However, the relative proton affinity of SiS and SiO for protonation at silicon could not be discerned. Moreover, the oxygen-site proton affinity of CO appears to be greater than the sulfur-site proton affinity of CS and the silicon-site proton affinity of SiO, all contrary to the indications of the more rigorous ab initio molecular orbital theory.

TABLE V: Computed and Experimental Proton Affinities (in kcal mol^{-1}) for CO and CS

molecule (site of protonatn)	computed PA	level	exptl PA
CO (C)	143.2[a]	MP4/6-311G**//6-311G**	141.9[b]
CO (O)	102.8[a]	MP4/6-311G**//6-311G**	102[c]
CS (C)	189.7[d]	CEPA-1	188.2[e]
CS (S)	115.4[f]	MRD-CI	

[a] At 298 K. Reference 32. [b] Reference 19. [c] Reference 26. [d] At 0 K. Botschwina, P.; Sebald, P. *J. Mol. Spectrosc.* **1985**, *110*, 1. [e] At 300 K. Smith and Adams, ref 12. [f] Semiempirical estimate at 298 K. Reference 12 and Pope, Hillier, and Guest, ref 33.

The computed net Mulliken charge condensed to each atom of the neutral base (Figure 2) is related to the magnitude and sign of the electrostatic potential in the close vicinity of that atom. With the exception of CO, proton attachment is seen to occur preferably to atoms which carry the greater net negative charge (Figure 2). The extent and direction of localization of net atomic charge in an isolated heteronuclear diatomic molecule is also associated with its permanent dipole moment. The relationship is only qualitative since the true magnitudes and positions of maximum negative and positive net charge density are not coincident with the atom positions, nor are the total net Mulliken charges condensed to atoms necessarily representative of their relative valence electron densities. However, the apparent deviance of CO is consistent with the failure of SCF level calculations to predict the correct sign of the small experimental dipole moment for this molecule, μ_D = 0.11 D in the direction $-C\equiv O^+$.[35] The corrected direction of net charge localization for CO concurs with the most stable configuration for protonated carbon monoxide. The net charges on the atoms of SiO, SiS and CS suggest that the oxygen-site proton affinity of SiO should be greater than the proton affinities of any of the molecules in this study, in agreement with higher levels of theory and with experiment. By similar reasoning, the following ordering of proton affinities is anticipated, SiS(Si) > SiO(Si), SiS(S) > CS(S), CS(C) > SiS(Si), and CS(C) > SiO(Si), and is verified by using more exact theory (Tables IV and V). Computed proton affinities gathered in these tables lie generally within ±2 kcal mol^{-1} of the experimental values where comparison is possible. A limitation of the simplistic conformity of net charge localization condensed to atoms with proton affinity is illustrated by the experimental discorrelation of the sulfur-site proton affinity of SiS and the carbon-site proton affinity of CS with the net Mulliken charges computed at the 6-31G** level of geometry optimization. This reversal may be due to an overestimation of the net Mulliken charge localization for SiS and an underestimation for CS, as suggested by a comparison of the theoretical dipole moments for SiS (2.44 D) and CS (1.34 D) with the experimental values of 1.73 ± 0.06 and 1.958 ± 0.005 D.[36,37] More likely, however, the discrepancy is due to employment of the net Mulliken charge density condensed to atoms as the sole

(31) $\Delta H_f(C_2H_3S^+)$ = 228 kcal mol^{-1} has been proposed by: Conde-Cabrace, G.; Collin, J. E. *Org. Mass Spectrom.* **1972**, *6*, 415. The ion was generated by electron-induced fragmentation of 1,3-dithiolane and by secondary fragmentation of $C_2H_4S^+$. Nearly identical MIKES spectra of $C_2H_3S^+$ have been obtained from a number of source molecules (Paradisi, C.; Scorrano, G.; Daolio, S.; Traldi, P. *Org. Mass Spectrom.* **1984**, *19*, 198) indicating a common structure for this ion. The thioacetyl structure CH_3CS^+ was ruled out because of the nonappearance of CH_3^+ on fragmentation. In contrast, SCF level calculations suggest that CH_3CS^+ is the lowest energy species of three likely isomers (Rodriquez, C. F.; Hopkinson, A. C. *Org. Mass Spectrom.* **1985**, *20*, 691). Consequently, −13.5 kcal mol^{-1} should be an upper limit to the exothermicity for hypothetical generation of CH_3CS^+ from the reaction of HCS^+ with CH_3SH at room temperature.

(32) DeFrees, D. J.; McLean, A. D. *J. Comput. Chem.* **1986**, *7*, 321.

(33) Pope, S. A.; Hillier, I. H.; Guest, M. F. *J. Am. Chem. Soc.* **1985**, *107*, 3789.

(34) Pauzat, F.; Talbi, D.; Ellinger, F. *Astron. Astrophys.* **1986**, *159*, 246.

(35) Raghavachari, K.; Pople, J. A. *Int. J. Quant. Chem.* **1981**, *20*, 1067.

(36) Hoeft, J.; Lovas, F. J.; Tiemann, E.; Torring, T. *Z. Naturforsch.* **1969**, *24a*, 1422.

(37) Winnewisser, G.; Cook, R. L. *J. Mol. Spectrosc.* **1968**, *28*, 266.

monitor of the thermochemistry. The permanent dipole will be greatly perturbed by induced polarization effects as the proton and base approach. Moreover, since the proton affinity of a base is equal to the enthalpy for deprotonation of the protonated molecule, the proton affinity is inherently associated with the base atom to hydrogen atom heterolytic bond strength. A quantitatively useful bearing of this feature is that the difference in proton affinities for bimodal proton attachment to the neutral base is equal to the difference in bimodal hydrogen atom affinities for the ionized base molecule.

Encouraging correlations of the qualitative ordering of the nitrogen-site and carbon-site proton affinities of homologous alkyl cyanides, isocyanides, and acetylenes, respectively, with various electrostatic and polarization properties of these molecules computed at a consistent level of theory have been made by Meot-Ner et al.[38,39] It is worthwhile in our study to investigate whether the variation of some of these properties computed at a consistent level of theory follows the ordering of proton affinities for pairs of molecules which protonate at the same atom and whose corresponding protonated ions bear the same principal molecular symmetry. These properties are delineated as follows.

μ_D, $\alpha_{\perp,\parallel}$. The permanent dipole moment, μ_D, and the polarizability, α, of a neutral base are related indirectly to the proton affinity via the classical electrostatic interaction potential. Moreover, because our study addresses bimodal proton affinities for each base, the direction of μ_D is as important as its magnitude. At orbital distances of approach or detachment of the proton, the induced dipole moment of the base will be fully aligned with the proton. Consequently α parallel to the molecular axis of a diatomic base, $\alpha_\parallel$, should govern the dipole moment induced during the generation of a linear ion, while α perpendicular to the internuclear axis, $\alpha_\perp$, should determine the moments induced during formation of the bent species CSH^+ and $SiSH^+$.

E(1s(B)). Molecular charge relaxation processes which accompany the ejection of a core 1s electron from oxygen or nitrogen among homologous alcohols or amines, respectively, have been shown to parallel changes in charge redistribution pursuant to protonation of the heteroatom.[40] The qualitative similarity of these perturbations in chemically similar environments effects a general and remarkably good correlation between the proton affinity of a molecule and the core 1s binding energy, E(1s(B)), of the atom to which proton attachment occurs.

Δq_T, Δq_s. A greater total electron density transferred from the base to the proton, Δq_T, should enhance the strength of the bond to hydrogen. Similarly, for the protonation of identical atoms, the amount of negative charge transferred from the substituent atom, Δq_s, by induction or polarization to bonding orbitals in the protonated base should enhance the strength of these bonds.[41]

E_σ, E_π. Δq_T and Δq_s are related to the energy and population of the highest molecular orbital of σ or π symmetry in the neutral base that is dominant in the formation of the bond to hydrogen. The relative valence electron density on the donating base atom in this orbital can be gleaned from the Mulliken orbital population analysis.

CO and CS. These bases are protonated at the carbon end in the ground state and both protonated molecules possess linear geometry (Figure 2). The normal order of their proton affinities, PA[CS(C)] > PA[CO(C)], relates expectedly to differences in μ_D, Δq_T, Δq_s, E(1s(C)), and E_σ. Importantly, since E_σ(CS) > E_σ(CO), CS should be a better σ donor than CO through carbon. The amount of electron density transferred from the neutral to the proton in the corresponding molecular ions reflects opposing competition between the electronegativity and polarizability of O and S favoring, ultimately, the greater ability of the sulfur substituent atom to delocalize positive charge through the higher energy π molecular orbital (HOMO). This feature is common also to silicon-site protonation of SiO and SiS.

TABLE VI: Ionization Energies and Proton Affinities for a Sample of Bases Which Protonate at the Heteratom, and the Hydrogen-Atom Affinities of Their Ions

RX	IE[a]	ΔIE[a]	HA-(RX⁺)[b]	ΔHA-(RO⁺,RS⁺)[b]	PA[c]
H_2CS	9.44		88.8		184.7
H_2CO	10.88	1.44	109.0	20.2	171.7
CS_2	10.08		83.3		164.4
OCS	11.18	1.10	94.9	11.6	150.7
CH_3SH	9.44		91.5		187.4
CH_3OH	10.85	1.41	118.5	27.0	181.9
$(CH_3)_2S$	8.69		87.4		200.6
$(CH_3)_2O$	9.94	1.25	107.7	20.3	192.1

[a] Adiabatic ionization energies at 0 K in eV, compiled from ref 24. IE = $\Delta H_f°_0(RX^+) - \Delta H_f°_0(RX)$. ΔIE = IE(RO) − IE(RS). [b] Hydrogen-atom affinity at 298 K in kcal mol^{-1} obtained from the approximate relationship $PA_{298}(RX) \simeq HA_{298}(RX^+) + IE_0(H) - IE_0(RX)$. [c] Proton affinity at 298 K in kcal mol^{-1} compiled from ref 19.

SiO and SiS. Protonation of SiO and SiS at silicon generates linear ions. The order of the computed silicon-site proton affinities of SiO and SiS correlates with monotonic changes in $\alpha_\parallel$, Δq_T, Δq_s, and E_σ while μ_D and E(1s(Si)) both discorrelate. The apparent discrepancy of μ_D is expected since proton attachment is forced to occur at electrostatically repulsive sites on both molecules. Consequently, electrostatic arguments could favor the larger enthalpy for proton attachment at silicon to be associated with the site bearing the smaller net positive charge and, by inference, the smaller dipole moment for the neutral molecule. Polarization effects indicate that sulfur has delocalized significant negative charge in $HSiS^+$ through the higher energy π (HOMO), Δq_s = 0.469, relative to the charge dispersed from oxygen in $HSiO^+$, Δq_s = 0.23. The order of this delocalization appears to reflect in the relative enthalpies of deprotonation of these ions (Table IV).

CS and SiS. CS and SiS protonated on sulfur generate bent ions with a bond angle of ~90°. It seems likely that the HOMO's of these bases effective in the formation of CSH^+ and $SiSH^+$ are of π symmetry. The sulfur-site proton affinity order SiS(S) > CS(S) is consistent with changes in $\sigma_\perp$, Δq_T, Δq_s, E(1s(S)), E_π, and μ_D (μ_D(CS) is opposite in direction to (SiS)). The order of E_π suggests that SiS may form stronger π complexes than CS with small positive atomic ions or with Lewis acids, while the order of Δq_s follows from the relative electronegativities of C and Si.

CO and SiO. Linear ions are generated from oxygen-site protonation of CO and SiO. Therefore, the effective HOMO's of these bases are of σ symmetry. The order of oxygen-site proton affinities is in accord with the trend of all of the molecular properties employed for these two molecules.

Interestingly, while the proton affinity of the sulfur site of CS is greater than that of the oxygen site of CO, the order is reversed for the silicon analogues. Within the qualitative analysis presented here, this reversal is best understood in terms of the anomalous hydrogen-atom affinity of SiO^+. Inspection of the normal order of heteroatom terminal proton affinities for a sample of organic oxides and sulfides is given in Table VI. Differences in the proton affinities of RS and RO analogues can be decomposed into the contributions from several terms

$$\Delta PA(RS,RO) = HA(RS^+) - HA(RO^+) - IE(RS) + IE(RO) \quad (8)$$

(38) Meot-Ner, M.; Karpas, Z.; Deakyne, C. A. *J. Am. Chem. Soc.* **1986**, *108*, 3913 and references therein.
(39) Deakyne, C. A.; Meot-Ner, M.; Buckley, T. J.; Metz, R. *J. Chem. Phys.* **1987**, *86*, 2334.
(40) Martin, R. L.; Shirley, D. A. *J. Am. Chem. Soc.* **1974**, *96*, 5299.
(41) Though the direction of net charge localization in CO is incorrect at the 6-31G** level of optimization, we have included this base in our overall qualitative scheme. The predicted *absolute* value for the dipole moment of the molecule is small which is in fair agreement with experiment. Additionally, computed dipole moments are critically dependent on the size and type of basis set employed. Therefore, it would be meaningless to compare shifts of charge localization among bases that are derived from different levels of theory.
(42) Derived from the experimental oxygen site PA(CO) at 303 K, Table V, and the experimental $IE°_0[(CO)-(H)]$ = 0.415 eV, ref 23.
(43) Murad, E. *J. Chem. Phys.* **1981**, *75*, 4080.
(44) Lias, S. G.; Ausloos, P. *J. Am. Chem. Soc.* **1978**, *100*, 6027.
(45) Colbourn, E. A.; Dyke, J. M.; Lee, E. P. F., Morris, A.; Trickle, I. R. *Mol. Phys.* **1978**, *35*, 873.

where all terms refer to 298 K and IE is the adiabatic ionization energy.[46] It is seen from Table VI that oxygen-containing bases always have higher ionization energies than their sulfur counterparts and ΔIE(RO,RS) varies from 1.10 to 1.44 eV. Moreover, the ionization energy differences are always greater than corresponding differences in the hydrogen-atom affinities, ΔHA, of oxide and sulfide ions. The ΔIE term therefore dominates the usual proton affinity order of oxide and sulfide bases and PA(RS) > PA(RO).

Using our kinetically bracketed proton affinity of SiS, 170.3 ± 2.0 kcal mol^{-1}, and IE(SiS) = 10.26 eV[7] we derive that the normal HA(SiS$^+$) = 93.3 ± 3.0 kcal mol^{-1} is in good agreement with the average HA(RS$^+$) = 88 ± 5 kcal mol^{-1} for the sulfur-protonated bases in Table VI. Moreover, ΔIE(SiO,SiS) = 1.35 eV[7,45] and is typical of the ionization energy differences among the sample of organic oxides and sulfides in Table VI. The heteroatom-site proton affinity order for SiO and SiS resolves, therefore, to the exceptionally large HA(SiO$^+$) = 143.4 ± 2.8 kcal mol^{-1}. This enthalpy is considerably larger than the average HA(RO$^+$) = 108 ± 12 kcal mol^{-1} or the empirical ΔH(CO$^+$–H) = 112 kcal mol^{-1}.[42] In fact, HA(SiO$^+$) appears to be more representative of the metal oxide ions for which HA(MgO$^+$) = 133.7 ± 18.5, HA(CaO$^+$) = 149.9 ± 13.8, HA(SrO$^+$) = 140.7 ± 9.2, and HA(BaO$^+$) = 133.7 ± 9.2 kcal mol^{-1} all at 0 K.[43]

The proton affinities of metal oxides range from 235 to 345 kcal mol^{-1} [19] and the normal proton affinity of SiO falls short of that range. Presumably the heteroatom–terminal proton affinity of silicon oxide reflects silicon's intermediate position in the periodic table. Whether the relative order of heteroatom-site proton affinities for SiO and SiS is representative of a general order for metal monoxides and monosulfides remains a topic for future experimental and theoretical investigations.

Acknowledgment. We thank the Natural Sciences and Engineering Research Council of Canada for financial support and Mr. John Houghton (Matheson Gases, Whitby, Ontario) who performed the purity analysis for allene.

Registry No. H$^+$, 12408-02-5; SiO, 10097-28-6; SiS, 113443-18-8; HOSi$^+$, 66106-76-1; HSSi$^+$, 76274-50-5; NH_3, 7664-41-7; HCN, 74-90-8; H_2S, 7783-06-4; H_2O, 7732-18-5; C_2H_4, 74-85-1; $(CH_3)_2O$, 115-10-6; CH_3COOH, 64-19-7; CH_3CN, 75-05-8; C_2H_5OH, 64-17-5; H_2C-CCH_2, 463-49-0; CH_3OH, 67-56-1; HCOOH, 64-18-6; CO, 630-08-0; CS, 2944-05-0.

(46) Adiabatic ionization enthalpies for a sample of organic molecules at 350 K, IH_{350}, differ rarely from extensively compiled adiabatic ionization energies at 0 K, $IE°_0$, by more than 0.05 eV.[44] Applying the stationary electron convention, it follows that the same difference should pertain to ionization energies at 350 and 0 K, and is likely to cancel in the term $IE°_0$-[(RO)–(RS)]. Therefore, $IE°_0$[(RO)–(RS)] can substitute for $IE°_{298}$-[(RO)–(RS)] when only qualitative comparisons of the latter property are required or when approximate values HA[(RS$^+$)–(RO$^+$)] are derived from PA[(RS)–(RO)].

Corrected Effective Medium Method. 3. Application to Clusters of Mg and Cu

Joel D. Kress,[†] Mark S. Stave, and Andrew E. DePristo*[,‡]

Ames Laboratory—USDOE and Department of Chemistry, Iowa State University, Ames, Iowa 50011
(Received: June 20, 1988)

We present a number of new concepts in the recently developed corrected effective medium (CEM) theory. First, the general CEM theory is specialized to the case of an infinite periodic three-dimensional solid. Second, construction of a covalent embedding function of the electron density from diatomic and bulk binding potentials is detailed. On the basis of the smoothness of the function in interpolation between the (low density) diatomic and (high density) bulk limits, we argue that this function is dependent only on the types of atoms in a system and not on the number of atoms in the system (i.e., a universal function of the electron density for particular types of atoms). Applications are made to the description of the structures and energies of homogeneous metal clusters containing from 2 to 201 atoms. Predictions of the equilibrium structures and energies of various high-symmetry structures of Mg_3, Mg_4, Cu_3, Cu_4, Cu_5, Cu_{13}, and Cu_{79} are compared to a number of ab initio and SCF-LSD results. The agreement is quite good even for the small clusters and becomes essentially perfect by Cu_{13}. Selected two-dimensional distortions of four-, five-, and seven-atom clusters are considered in detail, with the energetics presented via contour plots. These enable the determination of barriers to isomerization and/or the existence of especially floppy modes of the metal cluster. Geometrical optimization is performed for various configurations of Mg_{3-6}, Cu_{3-14}, and Cu_{19}. These accurate calculations on this range of clusters enable us to investigate the structural stability of the larger metal clusters for the first time. For still larger clusters of up to 201 atoms, we present binding energies for "spherical" bulk fragments to determine the onset of bulk binding.

I. Introduction

Investigations of the structural and energetic characteristics of small metal and semiconductor clusters is an active area of theoretical[1-20] and experimental[21-30] research. Much work has been directed toward the calculation of the most stable geometries of small clusters in high-symmetry arrangements, A_N with $N \approx 2$–13, by reasonably accurate ab initio or first-principle methods. Larger clusters have been treated by cruder semiempirical or ab initio methods that are not capable of accurate energy calculations. In both cases, the very interesting question of the kinetic barriers to the isomerization reactions in such clusters has not attracted much attention; the degree of "floppiness" of various cluster modes has not been considered in detail; and studies of the many lower

[†] Mobil Foundation and Henry Gilman predoctoral fellow. Present address: Group T-12, Mail Stop J569, Los Alamos National Laboratory, Los Alamos, NM 87545.

[‡] Camille and Henry Dreyfus Teacher–Scholar; Alfred P. Sloan fellow.

(1) See, for a general review; Koutecky, J.; Fantucci, P. *Chem. Rev.* **1986**, *86*, 539.
(2) Pacchioni, G.; Koutecky, J. *J. Chem. Phys.* **1982**, *77*, 5850.
(3) Jordan, K. D.; Simons J. *J. Chem. Phys.* **1980**, *72*, 2889.
(4) Chiles, R. A.; Dykstra, C. E.; Jordan, K. D. *J. Chem. Phys.* **1981**, *75*, 1044.
(5) Delley, B.; Ellis, D. E.; Freeman, A.; Baerends, E. J.; Post, D. *Phys. Rev. B* **1983**, *27*, 2132.
(6) Bachman, C.; Demuynck, J.; Veillard, A. *Faraday Symp. R. Soc.* **1980**, *14*, 269. In *Growth and Properties of Metal Clusters*; Bourdon, J., Ed.; Elsevier: Amsterdam, 1980.
(7) Flad, J.; Igel-Mann, G.; Preuss, H.; Stoll, H. *Chem. Phys.* **1984**, *90*, 257.
(8) Jeung, G. H.; Pelissier, M.; Barthelat, J. C. *Chem. Phys. Lett.* **1983**, *97*, 369.

0022-3654/89/2093-1556$01.50/0